



# Processing and characterization of aluminium alloys or composites exhibiting low-temperature or high-rate superplasticity

Jacob C. Huang

Institut of Materials Science and Engineering,  
National Sun Yat-Sen University, Kaohsiung, Taiwan, R.O.C.

Wide applications of superplastic forming still face several problems, one is the high temperature that promotes grain growth, another is the low forming rate that makes economically inefficient. The current study is intended to develop a series of fabrication and thermomechanical processing, so as to result in materials possessing either low temperature superplasticity (LTSP) or high rate superplasticity (HRSP). The former has been achieved in the cast Al alloys, while the latter was accomplished in powder-metallurgy aluminium matrix composites. The aluminium alloys, after special thermomechanical processes, exhibited LTSP from 300 to 450 °C with elongations varying from 300 to 700%. The LTSP sheets after 700% elongation at 350 °C still possessed fine grains 3.7 μm size and narrow surface solute depletion zones 11 μm in width, resulting in a post-SP T6 strength of 500 MPa, significantly higher than that of the HTSP superplasticity alloys tested at 525 °C or above. Meanwhile, it was found that LTSP materials may be transferred into HTSP materials simply by adding a preloading at 300-400 °C for a small amount of work. As for the endeavor in making HRSP materials, 2024Al/SiC, 6061Al/SiC and Al/Al<sub>3</sub>Ti systems processed by powder metallurgy or mechanical alloying methods are under investigation. The average sizes of the reinforcing SiC or Al<sub>3</sub>Ti particles, as well as the grain size are all around 1 μm. The aluminium composites have exhibited HRSP at 525-620 °C and 10<sup>-2</sup>-10<sup>1</sup> s<sup>-1</sup>, with elongations varying from 150 to 350%. This ultimate goal is to produce an alloy or composite exhibiting low temperature and high strain rate superplasticity (LT&HRSP).

## INTRODUCTION

### 1. Superplasticity:

Superplasticity is referred to the capability of certain polycrystalline materials to undergo extensive elongation, often preventing from continuous necking, prior to failure when tested at appropriate temperature and strain rates.

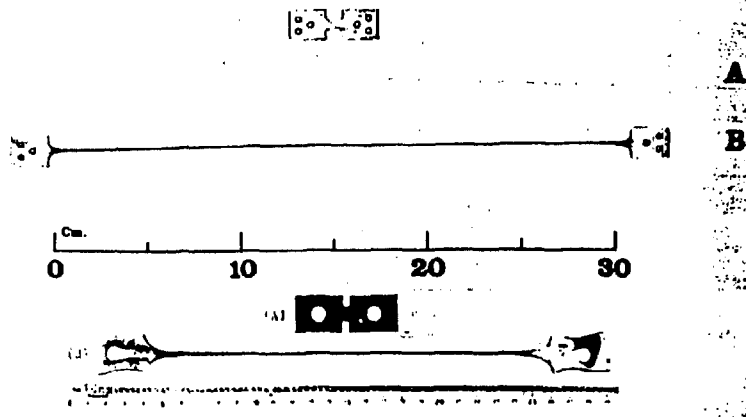


FIG. 1. A superplastic elongation of 4,850% is demonstrated in a Pb-62 wt% Sn alloy<sup>110</sup> by the two top samples and 5,500% is demonstrated by the two bottom samples in a commercial aluminum bronze.<sup>111</sup> The current world record is about 8,000% in the commercial aluminum bronze.<sup>111</sup>

## Processing and Characterization of Aluminum Alloys or Composites Exhibiting Low-Temperature or High-Rate Superplasticity

Jacob C. Huang

Institute of Materials Sci. and Eng.  
National Sun Yat-Sen University,  
Kaohsiung, Taiwan, R.O.C.

## Records of superplasticity

## HISTORICAL DATA ON SUPERPLASTICITY

Materials classification	Material	Elongation
Metals	Zn-Al	8800%
Metal matrix composites	6061Al/SiC	1400%
Intermetallic compounds	Super $\alpha_2$ Ti <sub>3</sub> Al	1500%
Supercooled amorphous mater.	La <sub>55</sub> Al <sub>25</sub> Ni <sub>20</sub>	15000%
Structure ceramics	Y-TZP	800%
High T <sub>c</sub> ceramics	Y-Ba-Cu-O	110%
Ceramic matrix composites	Al <sub>2</sub> O <sub>3</sub> /Y-TZ	625%
High rate superplastic mater.	MA-Al	1250%

1912 Bengough,  $\alpha + \beta$  Brass, approx. 200% elong.

1920 Resenheim et al., Zn-Al-Cu in near-eutectic composition

1928 Jenkins, Cd-Zn and Sn-Pb alloys, approx. 400% elong.

1934 Pearson, Pb-Sn and Bi-Sn eutectic alloys, 1950% elong.

1945 Sviderskaya, Zn-Al alloys, observed large elongations 'sverkhplastichnost' (ultra-high plasticity) was coined and led the term superplasticity became public

1962 Underwood, review paper, led to interest in Western world

1970 Commercial applications, non-structural

1974 Ti SPF applications, B-1 and Space Shuttle

1981 Guinness Book of Word Records, 4850% cong. in Sn-38Pb (Ahmed and Langdon, USC)

1985 Higashi, ~8000% elong. in Cu-Sn

1994 Langdon, ~8800% elong. in Zn-Al

# GBS ( Grain Boundary Sliding )

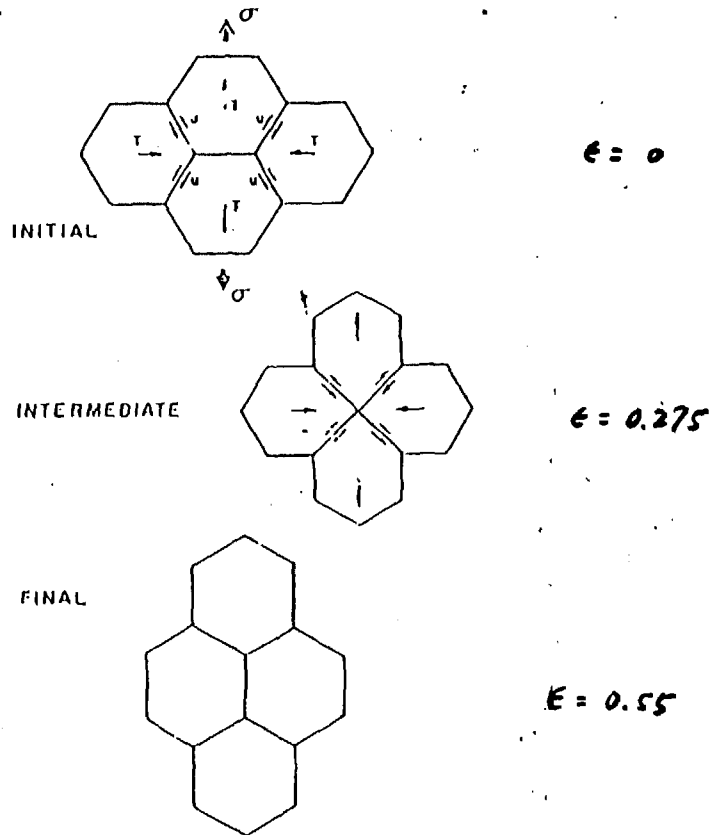


FIG. 2 A schematic illustration of the grain switching mechanism, involving grain boundary sliding, proposed by Ashby and Verall.

## Types of Superplasticity

- \* Micrograin superplasticity
  - Fully (or statically) recrystallized
  - Continuously (or dynamically) recrystallized
  - Requirement:
    - a. Fine and stable grain size (typically  $< 10 \mu\text{m}$ )
    - b. Temperature  $> 0.4T_m$
    - c. Controlled strain rate
    - d. Low flow stress
    - e. Low tendency for cavitation
    - f. High angle grain boundaries
    - g. grain size distribution
    - h. grain aspect ratio
- \* Transformation superplasticity
- \* Internal strain-induced superplasticity

formed Superform Metals Ltd and British Aluminium Company (now British Alcan Aluminium plc) began to produce the worlds first commercial superplastic aluminum alloy, Supral 100 (Registered Composition: Al, 6% Cu, 0.4% Zr; Designation: AA2004 produced per AMS4208). In 1974 Superform Metals Ltd introduced unique forming techniques and equipment (Reference 1) which enabled deep male formed parts to be produced. This male forming equipment is shown in Figure 2.

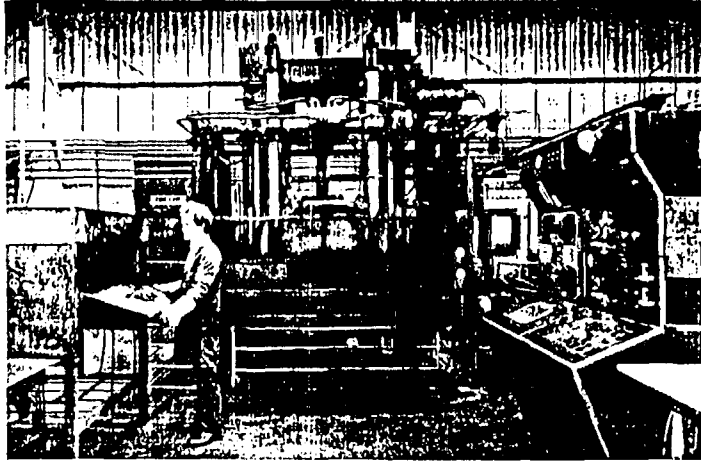


Figure 2 - Superform Male Forming Equipment

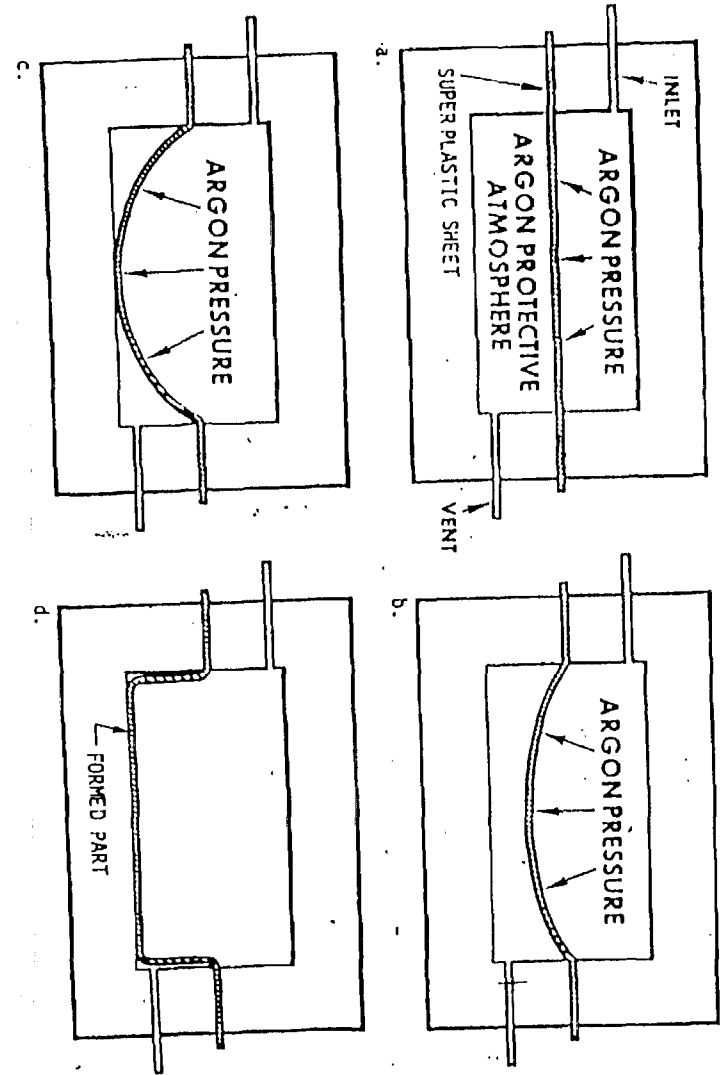
Detailed discussions of its operation has been covered elsewhere (Reference 2). The complete male forming process is illustrated by the progressive series of formings shown in Figure 3.



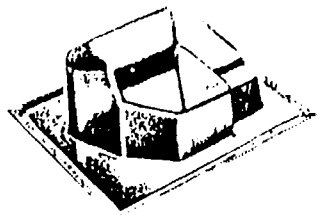
Figure 3 - The Complete Male Forming Cycle

- complicated shape
- one piece
- No string back
- low rate

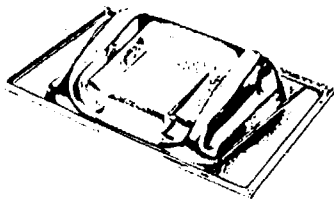
Fig 2-1



40% cost savings and improved dimensional accuracy compared with welded assemblies were achieved by the French Company, MESSIER HISPANO BUGATTI, by changing to SUPRAL. Four painted SUPRAL covers protect hydraulic pipe-work on the A300 Airbus undercarriage.



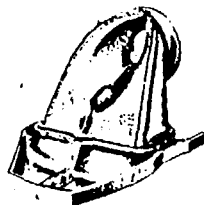
By selecting SUPRAL, M.L. AVIATION achieved greater consistency and interchangeability on the fairings for the Alpha Jet Store Carrier. More complex one piece shapes reduced hand finishing and avoided the distortion which could occur when welding drop-hammered or rubber pressed parts.



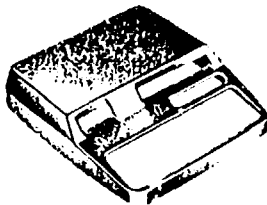
Increased life, simpler assembly and reduced costs were benefits gained by VICKERS MEDICAL when switching from glass fibre to SUPRAL inner bodies on infant incubator units.



Short lead times and ease of assembly were benefits gained when WESTLAND HELICOPTERS designed a new configuration engine intake for an experimental programme. The 35 piece riveted and welded construction was replaced from just 11 pressings which faithfully reproduced the master pattern.



An attractive design strong enough to withstand harsh industrial environments. Cooling against electrical noise and valuable heat sink properties were important benefits gained by SALTER INDUSTRIAL MEASUREMENTS on a weigh display unit.



SUPRAL panels form most of the external body work of the ASTON MARTIN LAGONDA giving distinctive lines and a reduction in hand finishing compared with rubber die pressed panels.

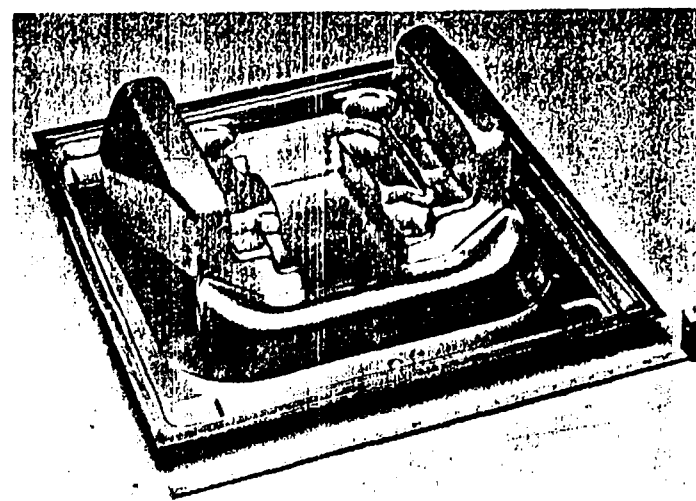
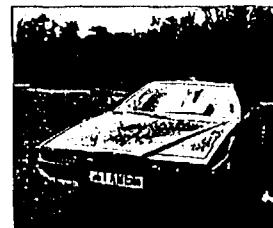
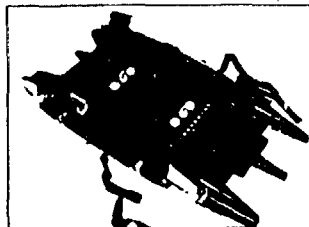
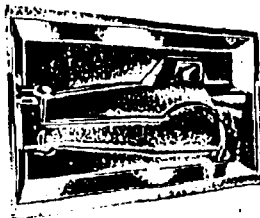


Figure 6 - Male Formed Ejector Seat Component Using Supral 100

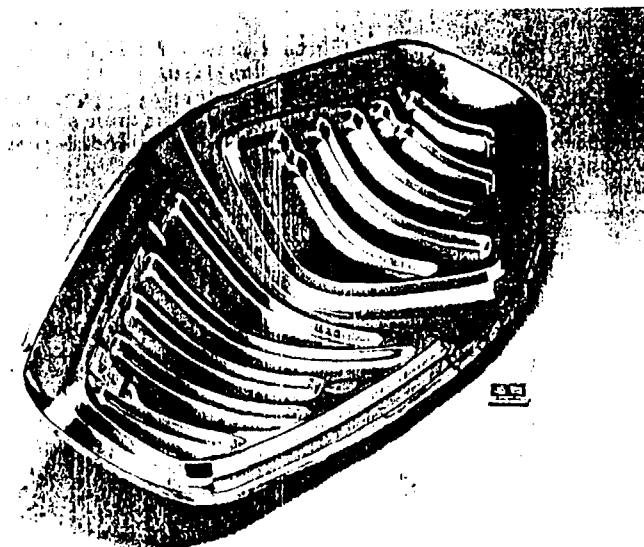
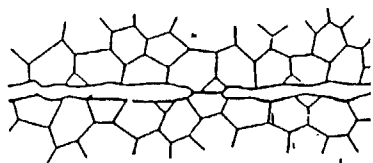
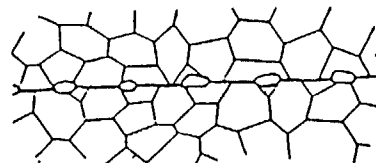


Figure 7 - Female Formed Pair of Helicopter Door Panels Using Supral 100

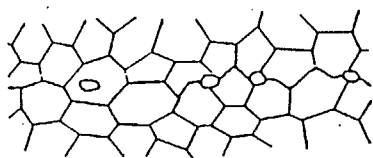
# Diffusion Bonding



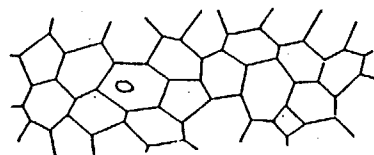
INITIAL:  
ASPERITY CONTACT



FIRST STAGE:  
DEFORMATION AND INTERFACIAL  
BOUNDARY FORMATION



SECOND STAGE:  
GRAIN BOUNDARY MIGRATION  
AND PORE ELIMINATION



THIRD STAGE:  
VOLUME DIFFUSION AND  
PORE ELIMINATION



## INTERMETALLIC BLADE (titanium-aluminum)

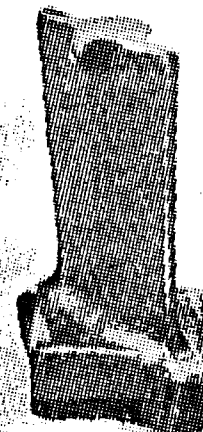
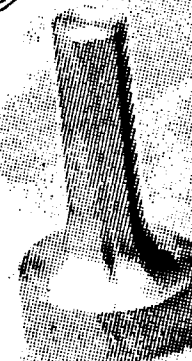
Blades are produced by superplastic forging out of the TiAl intermetallic alloy.

### Mechanical properties:

yield point, MPa	600
relative elongation	2.5%
fatigue limit	320

### Application:

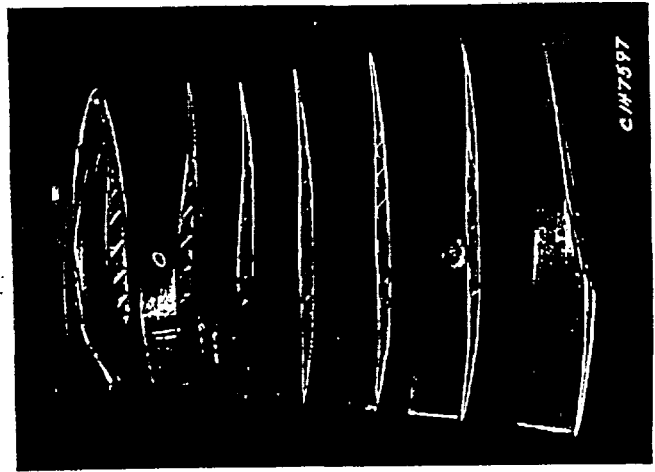
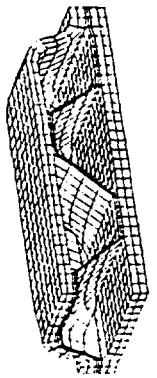
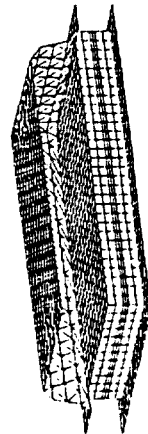
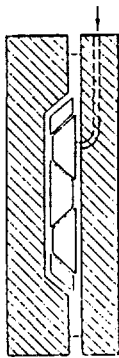
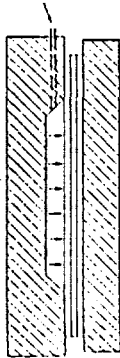
Blades are used in aircraft engines. The weight of gas-turbine engines with TiAl blades used in compressors decreases by 10-15%.



Prof. R. H. Chong

National Taiwan University

Taiwan, R.O.C



CIM7557

Three pieces

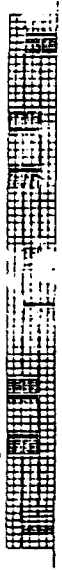
Prof. S. Lee

National

Central

University,

Taiwan, R.O.C



1.57e-03

8.45e-03

-1.25e-03

-1.80e-03

4.72e-03

3.18e-03

-8.00e-03

-2.10e-03

4.28e-03

-8.38e-03



-1.88e-02

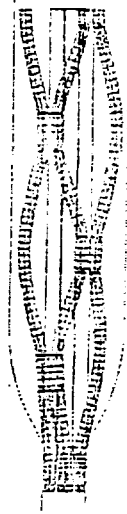
-3.25e-02

-4.96e-02

-8.00e-02

-8.27e-02

-9.31e-02



5.75e-03

3.50e-03

2.14e-03

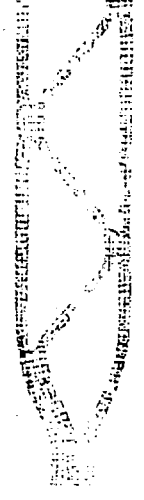
1.15e-03

-1.15e-03

-2.14e-03

-3.50e-03

-5.75e-03



(1.57e-03, 8.45e-03, -1.25e-03, -1.80e-03, 4.72e-03, 3.18e-03, -8.00e-03, -2.10e-03, 4.28e-03, -8.38e-03)



## Subject Covered

- \* Superplastic (SP) Materials Development:
  - (A) Aircraft-used and commercial aluminum alloys:
  - (B) Advanced materials, including aluminum matrix composites, intermetallic compounds:
    - Thermomechanical treatments (TMTs)
    - Modified powder metallurgy
    - Recrystallization routes
    - High-T and low-T; low-rate and high-rate SP
- \* SP Tensile Tests:
  - Constant crosshead speed and constant strain rate
  - With or without back pressure
  - Strain rate change
- \* Superplasticity Mechanism Analyses:
- \* Post-SP Characterization:
  - Microstructure characterization
  - Grain boundary sliding contribution
  - Mechanical property evaluation
- \* Superplastic Forming (SPF):
  - Forming system setup
  - SPF practices
  - Comparison between theories and experiments
  - Post-SPF property evaluation
- \* Computer Simulation:
- \* Joining for SP Thin Sheets:
  - Diffusion bonding
  - Electron-beam and laser-beam welding

*Prof. R. H. Cheng*

*National Taiwan University*

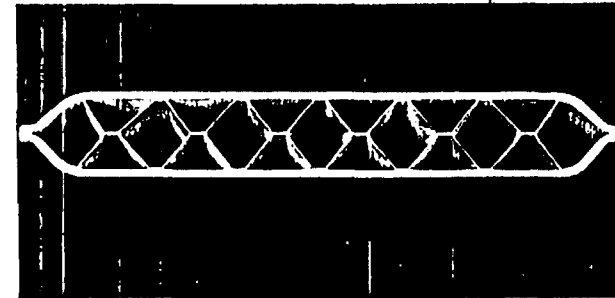


Figure 2 SPF/DB of titanium heat exchanger duct (Ref. 2).



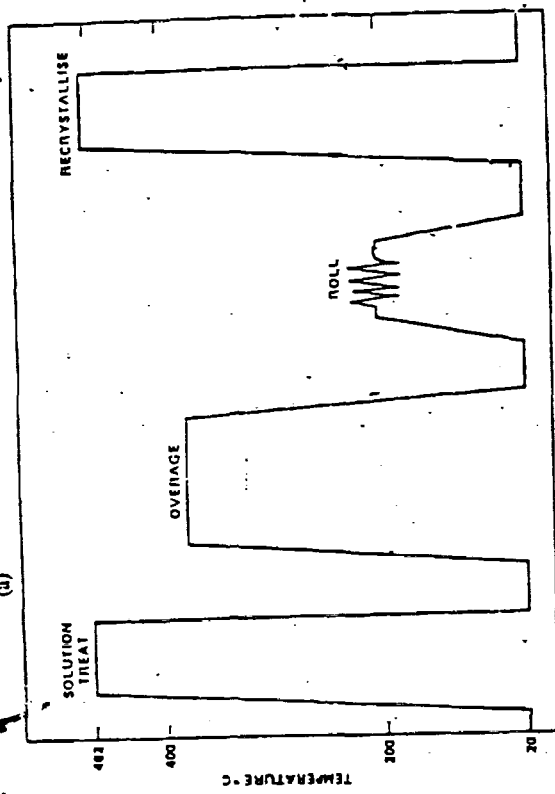
(d)

50 μm



(a)

1 μm



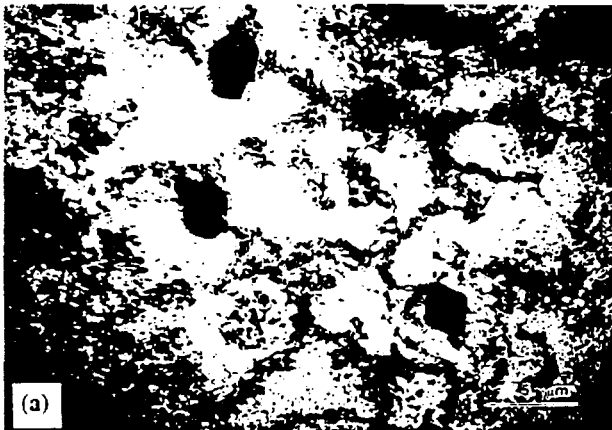
TIME

Fine grains

Coarse grains

Need:  
 ① Large particles ~ 1-2 μm to act as grain nucleation sites  
 ② Small particles ~ 0.1 μm to pin the grain boundaries

7 no 3 μm



(a)



(b)

Cr-rich particles  
 ~ 0.1 μm



(c)



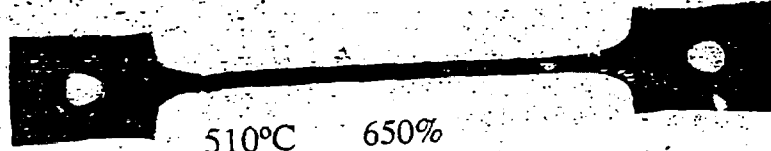
(d)

TEM micrographs of the precipitate and grain structure seen in the 7475 alloys: (a) large  $\eta$  precipitates in the as-rolled samples (b)-(d) small and stable grains and the Cr-rich particles. The pinning effect can be clearly seen in (c) and (d).

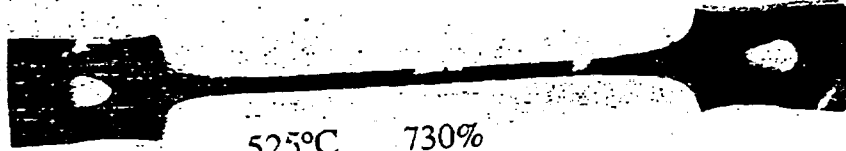
7475 Route 1 (Reheat time~ 15 min)



Not-deformed



510°C 650%



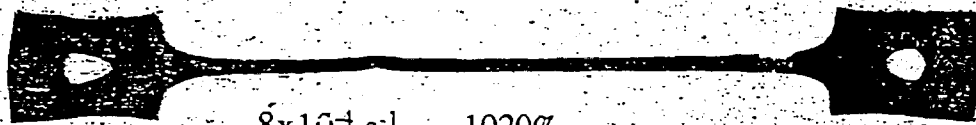
525°C 730%

Tensile elongations of 7475 route 1 for initial strain rate  $2 \times 10^{-4} \text{ s}^{-1}$  at different temperatures

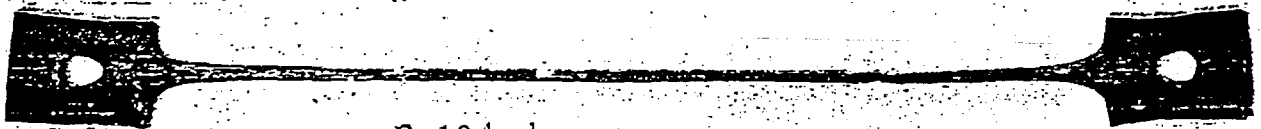
7475 Route 3 (Reheat time ~5 min)



Not-deformed



$8 \times 10^{-4} \text{ s}^{-1}$  1020%



$2 \times 10^{-4} \text{ s}^{-1}$  1500%

Tensile elongations of 7475 route 3 at different initial strain rates 510°C

The common working temperature for superplastic Al-Li alloys is

510-530 °C

(the high-temperature superplasticity, HTSP)

- \* Surface Li- and/or Mg-depletion zone to 100-200 μm
- \* Severe grain growth from the initial 5 μm to final 20 μm
- \* Appreciable cavitation associated with concurrent grain growth
- \* Degraded post-form RT mechanical properties

→ To develop

a superplastic Al-Li sheet with optimum working temperature of

350-450 °C

(the low-temperature superplasticity, LTSP)

★  
5083  
Al-Mg  
6061  
Al-Mg-Si

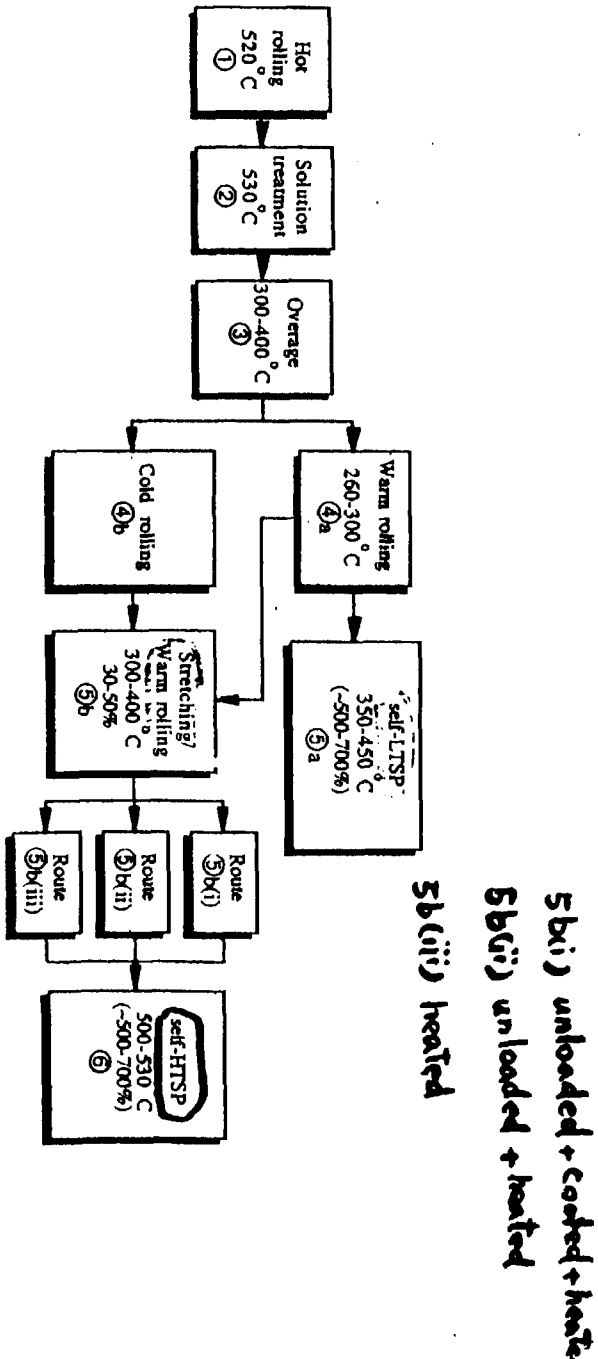


Fig. 1 Processing routes for producing the LTSP and HTSP thin sheets from a starting T3 thick plate.

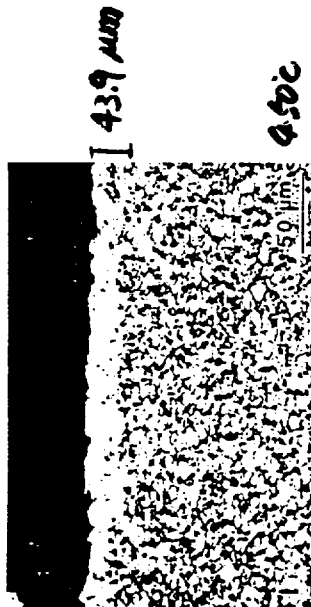
OM (in air)

~150%  
SP elongation

LTSP



LTSP



HTSP

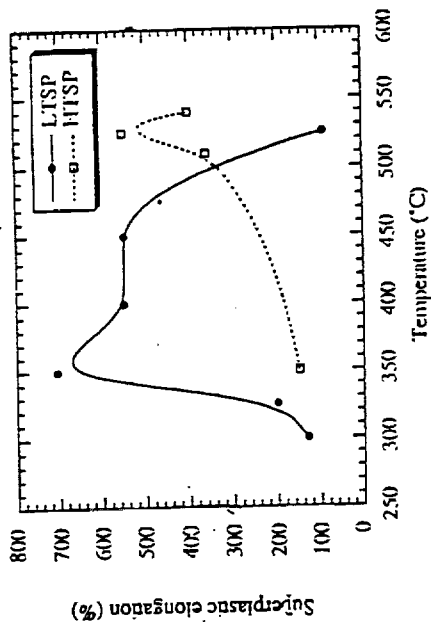


Fig. 1 The variation of superplastic elongations of the LTSP and HTSP sheets as a function of test temperature at an initial strain rate of  $8 \times 10^{-4} \text{ s}^{-1}$ .

SEM 450x 185x



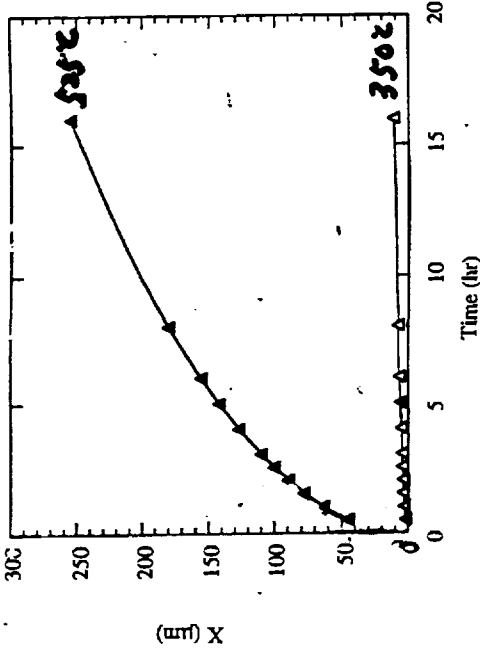
$R_{95} = 44 \pm 5\%$

350x, 200x

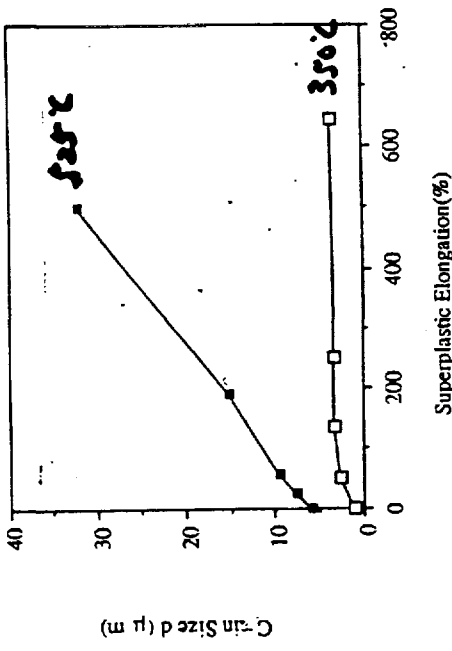
$R_{95} = 41 \pm 5\%$



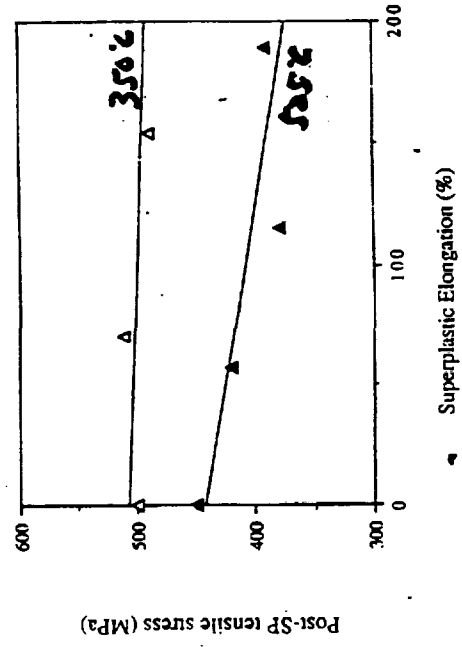
Li-dopamine

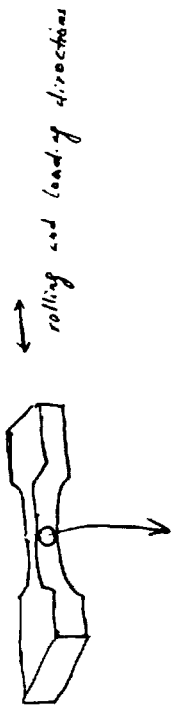


grain size



Post-SP  $\sigma_{ens}$





As-rolled.  
before SP



~100%

### Superplasticity in Metal Matrix Composites

For conventional superplastic alloys  $\dot{\epsilon} = 10^{-4} \sim 10^{-3} \text{ s}^{-1}$

For MMCs  $\dot{\epsilon} = 10^{-1} \sim 10^1 \text{ s}^{-1}$

Nieh et al. (1984)[1] first demonstrated

Nieh et al. (1991)[21] termed HSRS

High Strain Rate Superplasticity

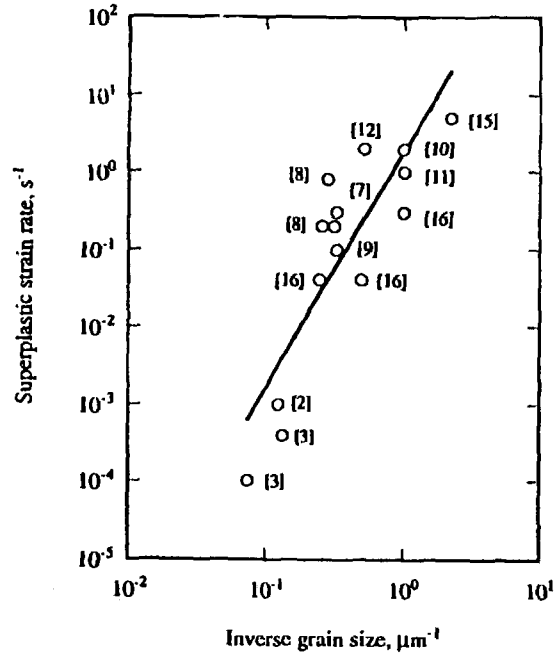


Figure 1 Grain size dependence of superplastic strain rate in aluminum matrix composites.

$$\dot{\epsilon} = A \frac{GbD}{kT} \left( \frac{b}{d} \right)^2 \left( \frac{\sigma - \sigma_0}{G} \right)^2$$

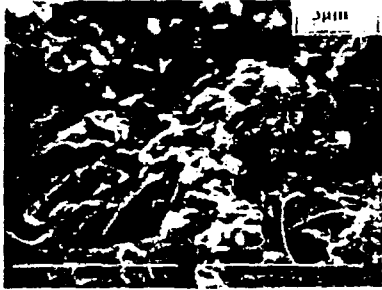
Table 1 Superplastic behavior in aluminum matrix composites

Composites	$\epsilon$ , %	$T_{sp}$ , °C	$\dot{\epsilon}$ , s <sup>-1</sup>	$m$	$d$ , $\mu\text{m}$
2124/SiC/20 <sub>w</sub> [1]	300	525	0.33	0.33	---
PM-64/SiC/10 <sub>p</sub> [2]	450	500	10 <sup>-3</sup>	0.5	8
2014/SiC/15 <sub>p</sub> [3]	160	480	10 <sup>-4</sup>	0.4	13.5
7475/SiC/15 <sub>p</sub> [3]	97	515	4x10 <sup>-4</sup>	0.43	7.3
2124/ $\beta$ -Si <sub>3</sub> N <sub>4</sub> <sub>w</sub> [4]	250	500	0.17	0.5	---
6061/ $\beta$ -Si <sub>3</sub> N <sub>4</sub> <sub>w</sub> [5]	200	525	0.16	0.5	---
6061/SiC/20 <sub>w</sub> [6]	300	550	0.17	0.32	---
6061/ $\alpha$ -Si <sub>3</sub> N <sub>4</sub> /20 <sub>w</sub> [7]	150	545	0.3	0.4	3
6061/ $\beta$ -Si <sub>3</sub> N <sub>4</sub> /20 <sub>w</sub> [7]	260	545	0.2	0.4	3.1
Al-Zn-Mg/ $\alpha$ -Si <sub>3</sub> N <sub>4</sub> /20 <sub>w</sub> [8]	160	525	0.8	0.4	3.5
Al-Zn-Mg/ $\beta$ -Si <sub>3</sub> N <sub>4</sub> /20 <sub>w</sub> [8]	230	545	0.2	0.4	3.8
6061/Si <sub>3</sub> N <sub>4</sub> /20 <sub>p</sub> [9]	450	545	0.1	0.3	3
6061/Si <sub>3</sub> N <sub>4</sub> /20 <sub>p</sub> [10]	620	560	2	0.3	1
5052/Si <sub>3</sub> N <sub>4</sub> /20 <sub>p</sub> [11]	700	545	1	0.3	1
6061/Si <sub>3</sub> N <sub>4</sub> /20 <sub>p</sub> [12]	500	560	2	0.5	1.9
6061/SiC/20 <sub>p</sub> [13]	207	580	0.27	0.33	---
6061/SiC/17.5 <sub>p</sub> [14]	350	580	0.1	0.5	---
IN9021/SiC/15 <sub>p</sub> [15]	610	550	5	0.5	0.45
2124/ $\beta$ -Si <sub>3</sub> N <sub>4</sub> /20 <sub>w</sub> [16]	280	545	0.04	0.3	4
2124/ $\beta$ -Si <sub>3</sub> N <sub>4</sub> /20 <sub>p</sub> [16]	280	500	0.3	0.3	1
2124/ $\beta$ -Si <sub>3</sub> N <sub>4</sub> /20 <sub>p</sub> [16]	840	515	0.04	0.3	2
6061/ $\beta$ -Si <sub>3</sub> N <sub>4</sub> /25 <sub>w</sub> [17]	173	545	0.02	0.3	---
7075/ $\alpha$ -Si <sub>3</sub> N <sub>4</sub> /27 <sub>w</sub> [18]	260	500	0.18	0.35	---
2024/ $\alpha$ -Si <sub>3</sub> N <sub>4</sub> /27 <sub>w</sub> [19]	175	500	0.17	0.3	---
2024/SiC/21 <sub>w</sub> [19]	140	510	0.09	0.38	---
8090/SiC <sub>p</sub> [20]	300	575	0.18	0.53	---

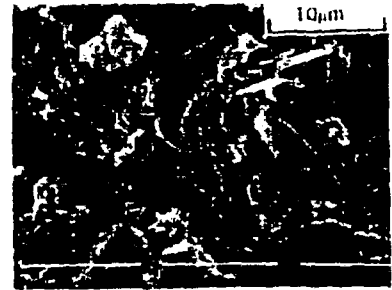


## Filament appearance on fractured surfaces

Hikosaka et al. [13]

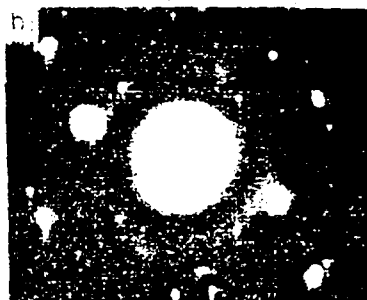


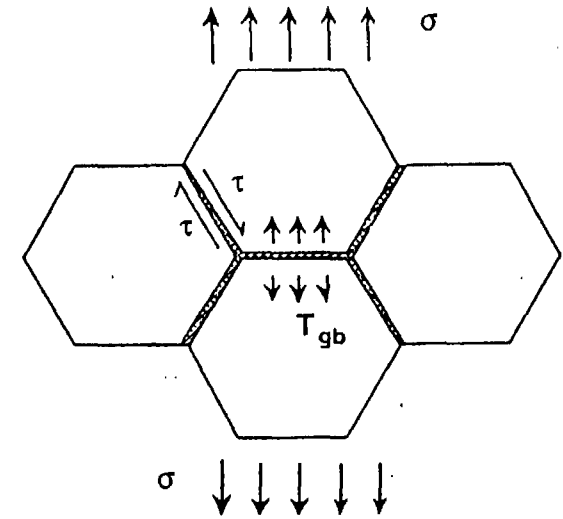
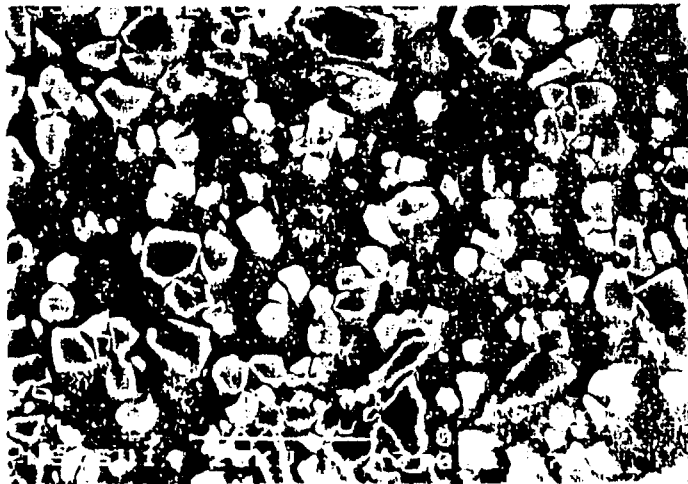
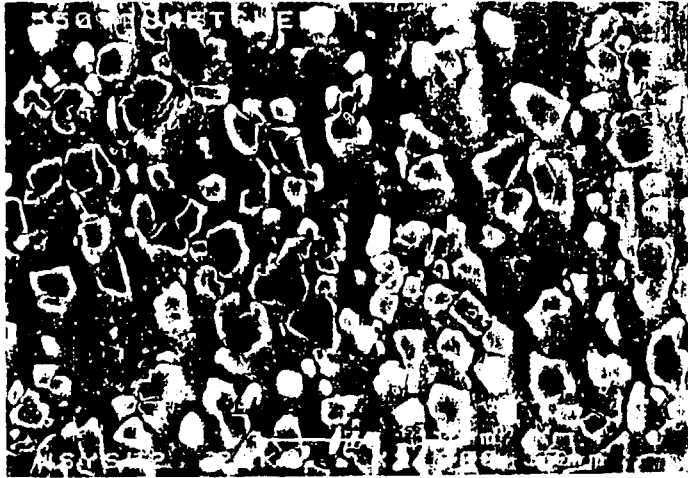
Nieh et al. [14]



Koike et al. [41] In situ observations in partial melting

Composites	$T_{sp}$	$T_i$	$T_s$
2124/Si <sub>3</sub> N <sub>4</sub> p	515	511	502
5052/Si <sub>3</sub> N <sub>4</sub> p	545	548	607
6061/Si <sub>3</sub> N <sub>4</sub> p	545	549	582

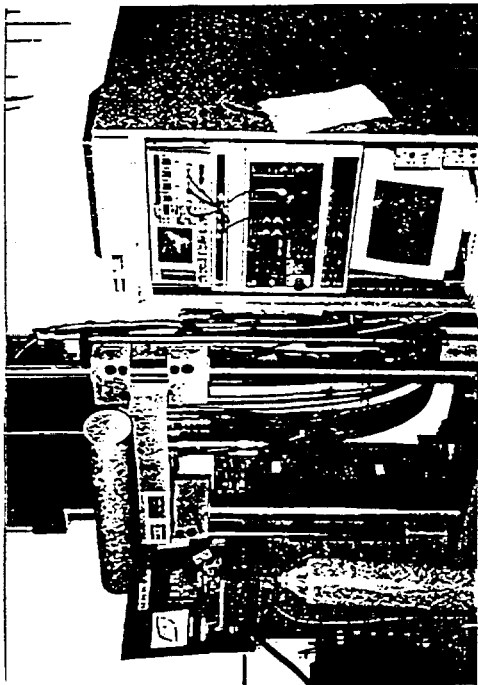




relieves stress concentration  
acts as lubricants

2024Al/15% SiC (p)

$d_p \sim 2.5 \mu m$



MTS  
819

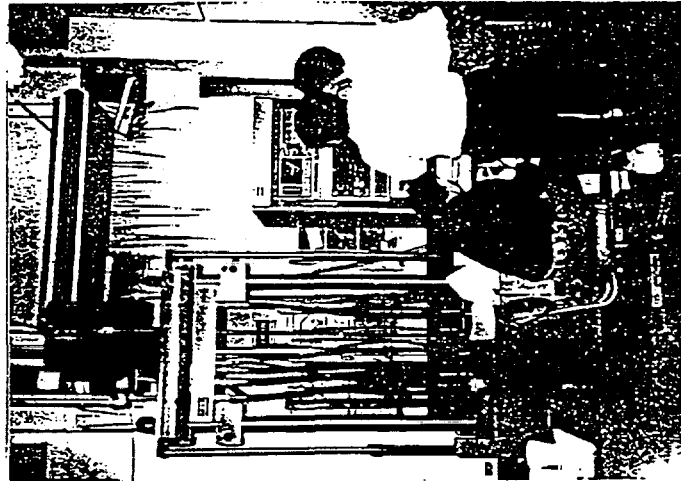
5-ton

servohydraulic

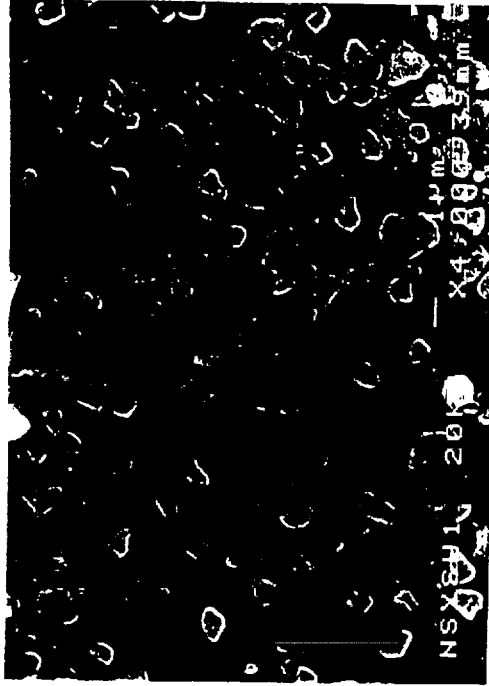
dynamic

high-rate

system



- \* Accumulator
- \* Kistler 9161A force link
- \* Kistler soap
- Charge amp
- \* LVDT
- \* Nicolet 420 oscilloscope
- \* Anti-rotation
- \* Tension, force Compression
- Punching
- Charpy, Bendin
- \* up to 16 m/s
- (E-15X16)
- \* HP. V66-Test Soft...



6061 Al / 15% SiC (p)

$d_p = 0.5 \pm 0.6 \mu m$

6061 Al / SiC ( $d \sim 0.03 \mu m$ )

6061 Al / Si ( $d \sim 0.03 \mu m$ )

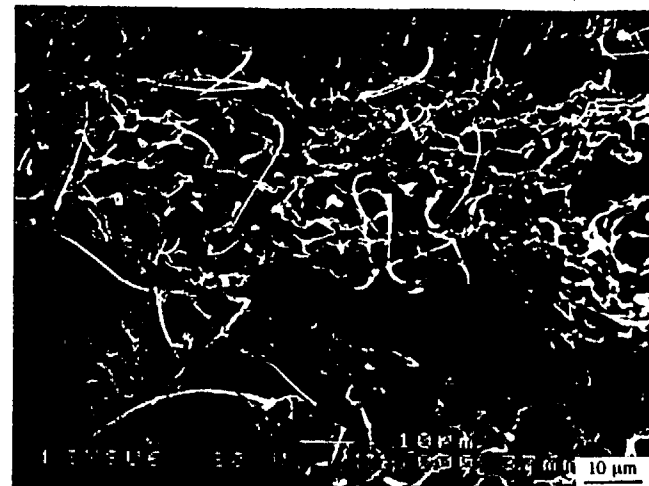
## Comparison of the test conditions and the optimum results obtained

	Particle size $d_p$ ( $\mu\text{m}$ )	Grain size $d$ ( $\mu\text{m}$ )	T ( $^{\circ}\text{C}$ )	$\dot{\epsilon}$ ( $\text{s}^{-1}$ )	$\epsilon$
7091/30% $\text{B}_4\text{C}$	5.0	5.0	545	$2 \times 10^{-2}$	110%
6061/15% SiC	2.5	3.5	580	$1 \times 10^{-2}$	150%
2024/15% SiC	2.5	3.5	525	$1 \times 10^{-1}$	167%
6061/15% SiC	0.5	0.8	525	$1 \times 10^{-1}$	286%
2024/15% SiC	0.5	0.8	580	$1 \times 10^{-1}$	230%
Pure-Al/ 15% SiC	0.5	0.8	640	$1 \times 10^0$	280%

6061/SiC 0.03 0.1

?

(a)



(b)

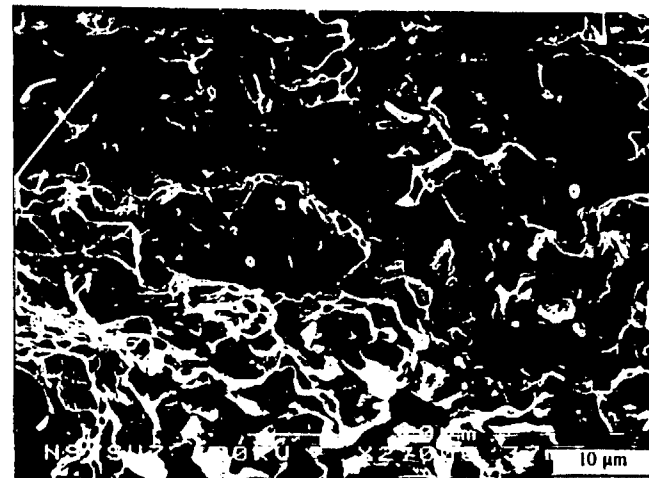


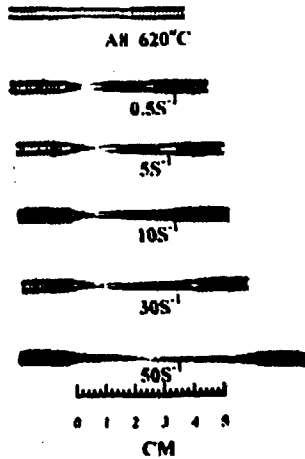
Fig. 43 SEM micrographs showing the (a) more extensive hair-like morphology, and (b) partial melting seen in the 6061 composite tested at  $580^{\circ}\text{C}$  at  $5 \times 10^{-4} \text{ s}^{-1}$ .

MA Al/Al<sub>3</sub>Ti

Prof. P. W. Kao

National Sun Yat-Sen University

A8	T (°C)	$\dot{\epsilon}$ (S <sup>-1</sup> )	$\epsilon$ (%)	$\Delta A$ (%)	U.T.S (MPa)	$\sigma_{0.1}$ (MPa)
	550		0.5	17	81	90
5			38	89	80	59
575		0.5	20	85	73	42
		5	55	92	78	63
		50	37	78	105	99
600		0.5	29	93	50	32
		5	50	92	70	51
		50	97	85	94	76
620		0.5	34	94	44	25
		5	65	94	45	29
		10	61	86	58	44
		30	94	86	63	57
		50	194	90	68	63



Al/Al<sub>3</sub>Ni

Lian, Chen, Liu (1997)

National Cheng-Kung University

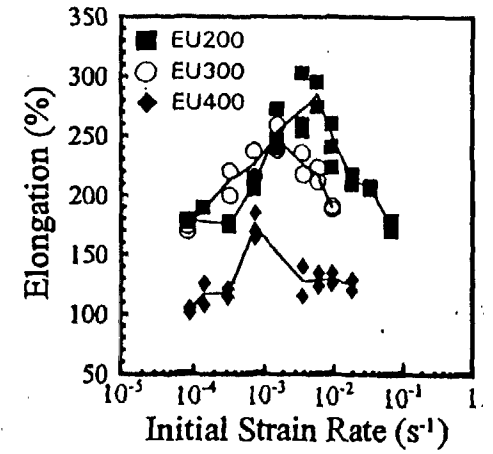
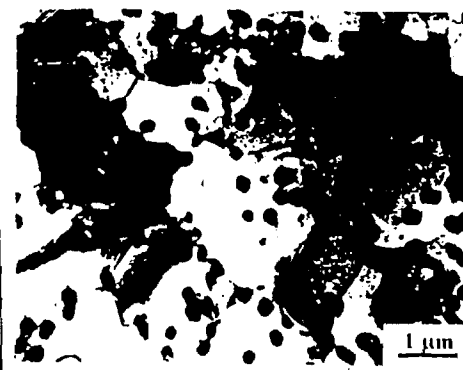
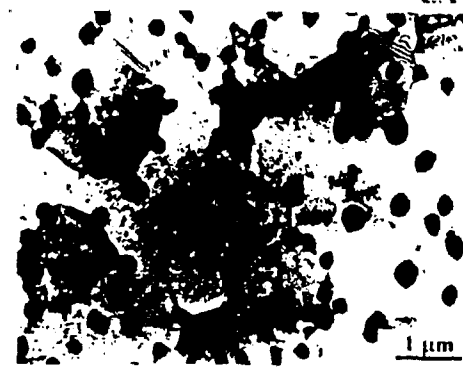
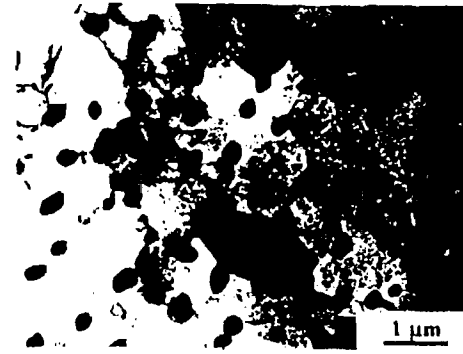


Fig. 3—Elongation as a function of initial strain rate for EU200, EU300, and EU400.

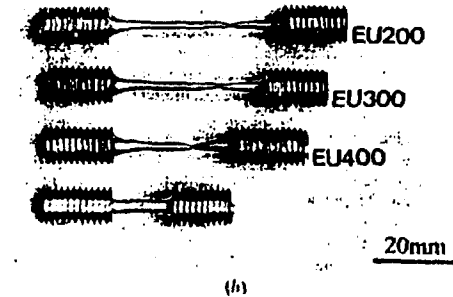


Fig. 4—(a) True tensile stress vs. true tensile strain and elongation of the three test materials obtained at their initial strain rates of maximum elongation. (b) Undeformed specimen and those deformed to failure at their initial strain rates of maximum elongation.

Fig. 5—TEM micrographs of the deformed specimens. (a) True stress section of EU200 at 10<sup>-3</sup> s<sup>-1</sup> and (b) EU300 at 10<sup>-3</sup> s<sup>-1</sup>.

Prof. J. W. Ye;  
National Tsinghua University

*Reciprocal Extrusion*

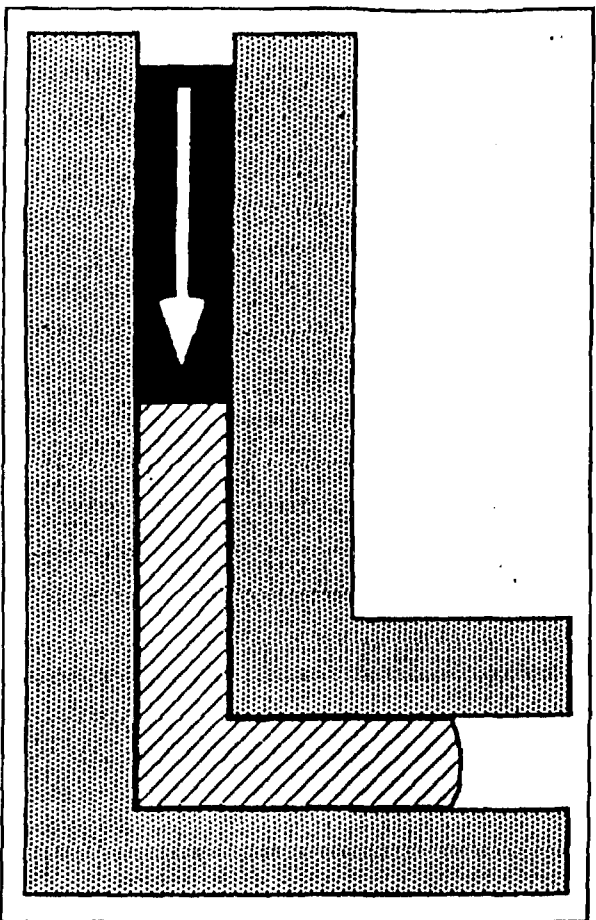
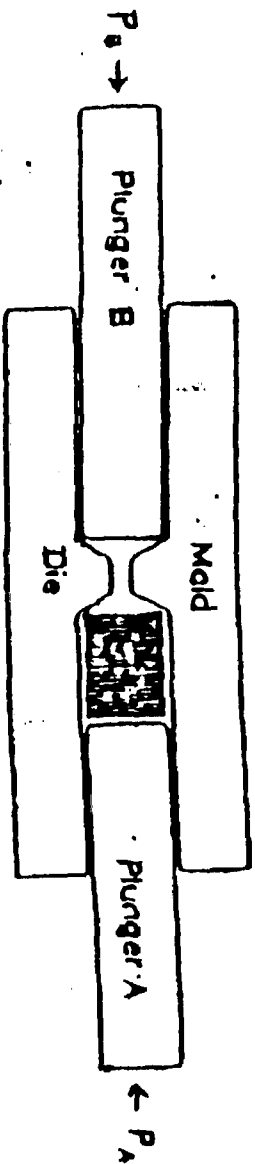


Figure 2. Equal channel area extrusion is a way to impart much working without causing a change in cross sectional area.<sup>37</sup>

Tsenev, Valiev, Kujeev (1997)

Parameters of superplastic deformation of alloys under study.

Alloy	d, $\mu\text{m}$	T, K	$\dot{\epsilon}$ , $\text{s}^{-1}$	$m = d \lg \sigma / d \lg \dot{\epsilon}$	$\delta$ , %	$\sigma_{20}$ , MPa
Al - Cu - Zr	8	773	$3 \cdot 10^{-3}$	0,50	800	6
	0,3	220%, 493	$3 \cdot 10^{-4}$	0,48	320	23
	8	493	$3 \cdot 10^{-4}$	0,19	130	34
Al alloy 1420	20	793	$4 \cdot 10^{-4}$	0,50	560	8,5
	0,8	340%, 573	$1 \cdot 10^{-4}$	0,41	330	15
Al alloy 1460	6	793	$3,5 \cdot 10^{-4}$	0,52	650	4
	0,9	330%, 603	$1 \cdot 10^{-4}$	0,37	370	12

T. R. McNelly and H. E. Matheson  
Naval Postgraduate School, USA

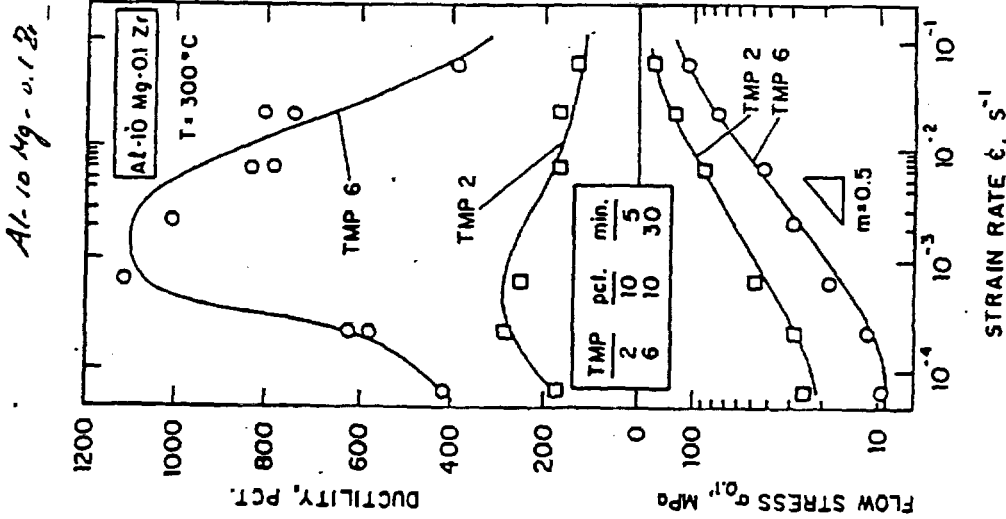


Fig. 1—Mechanical property data illustrating the variation in mechanical behavior at 300 °C for the two processing schedules.<sup>[5]</sup>

NEXT PAGE(S)  
left BLANK